FAILURE MECHANISM IN HIGH-STRENGTH CONCRETES

By

Gy. BALÁZS—J. BORJÁN

Department of Building Materials, Technical University, Budapest

Received May 31, 1977

1. Introduction

With the development of concrete industry, the share of precast high-strength concretes in the total concrete volume is increasing. Our previous research affected mostly the range of concrete grades B 200 to B 400.

Here the authors' experiments, made at the Department of Building Materials, Technical University, Budapest upon commission by the Concrete and Reinforced Concrete Works will be described [1]. Under axial load, the hardened concrete, a heterogeneous system of components with different properties and of voids undergoes axial compression nearly proportional to the compressive stress and at the same time a strain normal to the axis. In the ultimate condition, however, this proportionality vanishes. Ultimate strength is the maximum stress at failure, quotient of the ultimate force by the initial cross section area. This final state is preceded by a failure process. At 30 to 40% of the ultimate force already micro- then macro-cracks appear on the aggregate-paste interface, continuously increasing by number and by size until the concrete crushes and falls apart.

There are various methods, differing by principles, for examining the failure process, such as:

- analysis of the crack pattern in a concrete loaded to different degrees, then unloaded and sliced up;
- ultrasonic velocity determination;
- determination of noises caused by breakage;
- direct volumetric deformometry;
- measurement of surface deformations of the specimen;
- mathematical analysis of stresses in an elastic system of aggregate and cement mortar.

Our tests involved determination (and $X-Y$ plotting) of axial and transversal deformations in the midline of concrete prisms 36 cm high, as well as of the ultrasonic velocity normal to the force direction. Surface deformations were converted to volumetric deformations by the method of BÉRES [2], [3] and the results compared to ultrasonic test results.

2. The investigated concretes and their tests

Concretes of compositions seen in Table 1 were investigated.

Table I

Composition and 28-day cube strength of test concretes

Symbol	Cement grade	Cement dosage, kg/cu.m.	D_{max}, mm	Abram's modulus	w/c ratio	Cube strength, kg/sq. cm
1	T500	130	10	4.24	0.94	130
4	T500	100	40	5.04	0.90	128
5	T600	228	10	4.24	0.61	428
6	T600	210	20	4.50	0.64	418
8	T600	190	40	5.04	0.645	380
9	T600	300	10	4.24	0.43	610
10	T600	280	20	4.50	0.43	617
12	T600	260	40	5.04	0.52	532
13	T600	415	10	4.24	0.37	676
14	T600	390	20	4.50	0.40	695
16	T600	360	40	5.04	0.395	682
17	T600	530	10	4.24	0.317	756
18	T600	490	20	4.50	0.310	822
19	T600	490	20	4.50	0.310	824
20	T600	460	40	5.04	0.326	716
21	T600	660	10	4.24	0.277	814
22	T600	615	20	4.50	0.284	800
24	T600	570	40	5.04	0.289	795
25	T600	530	10	4.24	0.396	626
26	T600	530	10	4.24	0.356	673
27	T600	460	40	5.04	0.425	561
28	T600	460	40	5.04	0.375	610
29	T600	530	10	4.00	0.337	730
30	T600	460	40	5.80	0.293	684
31	T600	300	10	4.24	0.675	316
32	T600	300	10	4.24	0.550	444

Prism specimens 12 by 12 by 36 cm, one for each series, have been applied to determine the primary stress-strain diagram, three specimens were tested for the moduli of elasticity at about 30%, 60% and 90% of the prism strength, the total stress-strain diagram, and the transversal contraction coefficient (Fig. 1).

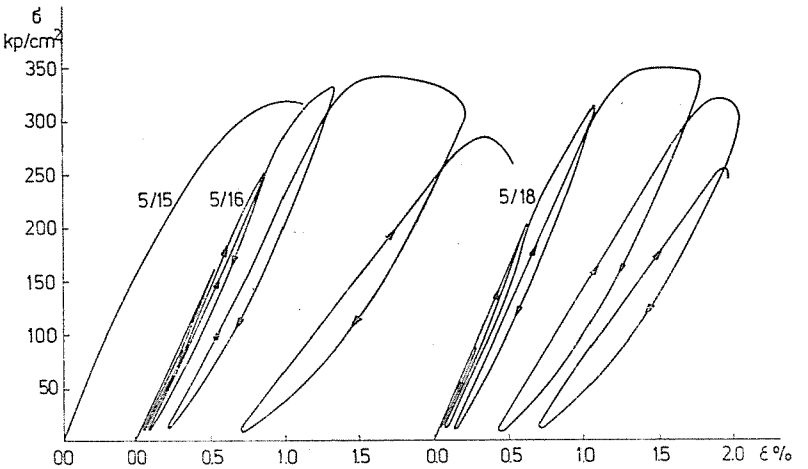

Fig. 1. Stress-compression curves of concrete specimens type 5

Stress-strain diagrams have been recorded by an induction strain gauge type Hottinger D-32 mounted on the halving line of two opposite prism faces and by an amplifier bridge, using an $X-Y$ recorder.

Ultrasonic measurements applied a so-called "betonoscope". The 500 kHz emitter-pickup head of the instrument was mounted in the transversal strain gauge plane. Velocity values were determined by means of a Schmidt discriminator incorporated in the instrument. This unit enhanced the slope of the impulse pattern on the oscilloscope screen, increasing the reading accuracy, and making the measured ultrasonic velocity amplitude-dependent.

Variation of the ultrasonic velocity has also been observed in unloading, and the residual velocity variations determined.

3. Analysis of volumetric deformations under load

According to Béres, "the lower limit of structural loosening for hardened concrete is the physical condition where the void volume reduction due to the closure of voids and cracks exhibits a limit value because of the opening of cracks". The lower limit of structural loosening is at the maximum of the function $d\Theta/d\sigma$, while the structural decomposition level resulting in the unstable condition is where the above function is zero.

Volumetric deformation due to elastic deformations is:

$$\Theta_{\text{elast.}} = \frac{\sigma}{E}(1 - 2\mu)$$

where

σ — instantaneous compressive stress, kp/cu.m

E — modulus of elasticity, kp/cu.m

ν — Poisson's ratio.

In case of elastic deformations, permanent variation of its derivative with respect to σ:

$$\frac{d\Theta_{\text{elast.}}}{d\sigma} = \frac{1-\mu}{E}$$

hints to the variation of the concrete voids volume.

Volumetric deformation functions Θ have been constructed by first plotting functions $\sigma_x - \varepsilon_x$ and $\sigma_x - \varepsilon_y$, then dividing them into 0.1 parts of the prism strength values σ_p on the σ/σ_p axis (Fig. 2). In the vicinity of failure, the divisions became denser. Approximate value of the volumetric deformation in each section has been computed:

$$\Delta\Theta = \Delta\varepsilon_x - 2\Delta\varepsilon_y$$

where $\Delta\varepsilon_x$ and $\Delta\varepsilon_y$ are increments of longitudinal and transversal deformations, respectively, along the tested section.

The computed values have been plotted as prism strength percentages in Fig. 2, showing also the procedure of construction.

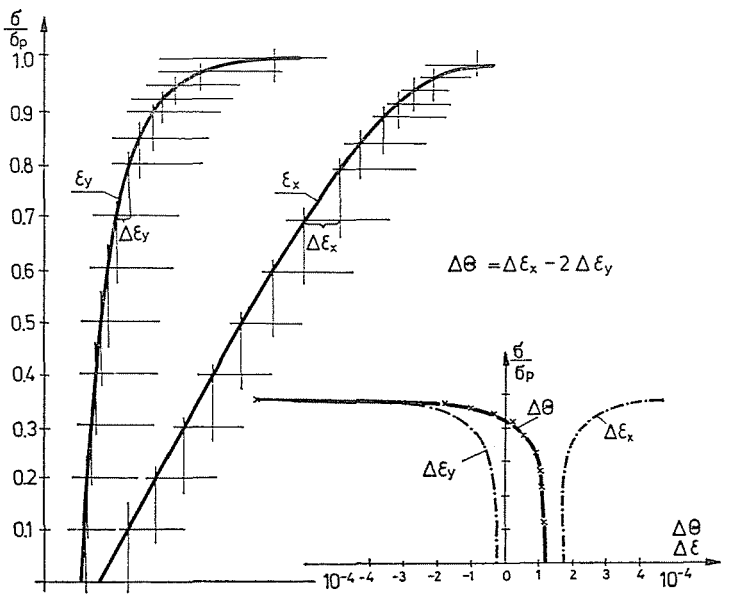

Fig. 2. Construction of volumetric deformation functions. Concrete No. 26

Part of the diagrams Θ had no typical maxima (Figs 1, 2), others had a marked maximum such as that in Fig. 3.

Typical points of characteristic Θ curves are:

1. Initial volume decrease
2. Start of volume decrease to intensify (deviation of curve Θ from the vertical)
3. Maximum volume decrease
4. Zero volume decrease.

Characteristics of curves Θ for single loadings have been compiled in Table 2.

According to the tests — in the range of high-strength concretes — point 2 is at 40%, point 3 at 60% and point 4 at 90% of the ultimate strength as an average.

Curves for several loading-unloading cycles are shown in Fig. 4.

Both deformation and volumetric deformation functions show a typical hysteresis, the volume deformation function is not zeroed sooner than immediately before failure.

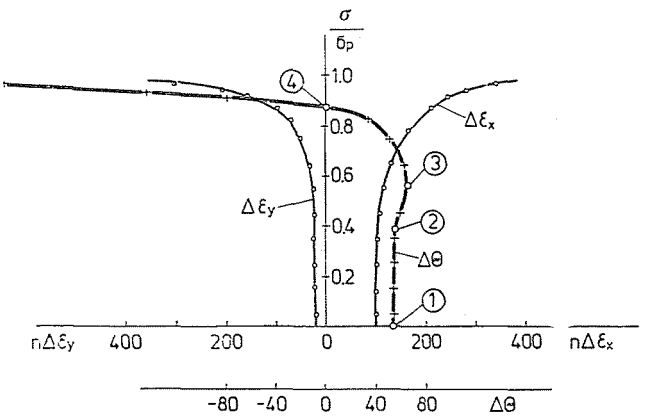

Fig. 3. Function Θ with a typical maximum, and its coherent points. Concrete No. 5.

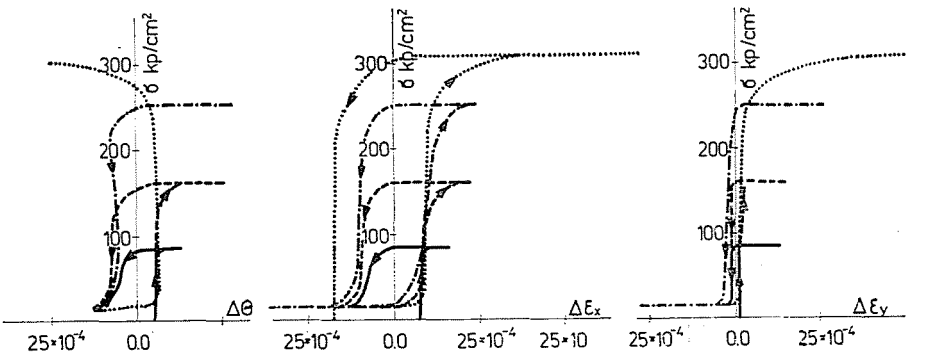

Fig. 4. Loading-unloading cycles. Concrete No. 32

Table II

Characteristic function points in terms of prism strength percentages

Concrete symbol	Initial 10^{-3}%	Stress causing volume decrease		Locus of $\Delta\Theta = 0$
		start	peak	
		100%		100%
Point symbol	1	2	3	4
1	30	25	80	93
4	34	15	55	86
5	54	35	55	87
6	70	—	25	92
9	61	70	93	98
10	40	50	87	97
12	90	—	10	85
13	40	35	60	80
14	48	30	45	80
16	105	50	83	93
17	100	20	60	93
18	127	30	45	79
20	90	20	75	—
22	60	35	60	86
24	120	—	25	94
25	70	—	45	80
26	110	—	46	84
27	85	40	70	90
28	80	50	60	90
29	110	—	45	99
30	80	—	45	79
31	75	45	87	96
32	80	70	90	98
Average	77	39	62	89

4. Ultrasonic tests of the failure mechanism

The testing betonoscope transfers longitudinal wave pulses into the concrete. The oscilloscope screen displays picture of pulses emerging from the emitter and taken up by the pickup, against a time scale. Spacing of the two signals is proportional to the propagation time. The pickup is excited by the earliest arriving wave front but there is an infinity of sound paths to carry the wave pulse, since in solid media other, mainly transversal waves are propagating, independent of the excitement method.

Acoustic resistance of voids and cracks is rather high compared to solid and water-filled voids, thus, in case of a crack or void across the theoretically shortest sound path (the common axis of emitter and pickup), the fastest longitudinal pulse does not attain the pickup. On the other hand, a signal hits partly as a longitudinal, and partly as a transversal wave, somehow bypassing the crack, and excites the pickup at a delay. Therefore the observed propagation velocity is only fictitious, an average computed from the passage time of most pulses, and of the specimen transversal size. Thereby arise and increase of cracks across the sound path are sensed as virtual velocity decrease.

The resonating branch of the natural wave pulse is a curve of a slope depending on the amplitude. The Schmidt discriminator is a tipping circuit with a tipping level considered as constant during one measurement. It is actuated by the natural wave pulse tension attaining the tipping level. The sound path increase due to crack development adds to acoustic losses, reducing the signal amplitude, thereupon the tipping circuit will act at a delay. Further virtual velocity decrease is due to the application of a Schmidt discriminator.

Fig. 5 shows two examples for the variation of the virtual propagation velocity according to the prism strength ratios. The figure in the right-hand side shows an unloading. Some typical examples of velocity curves are shown in Fig. 6.

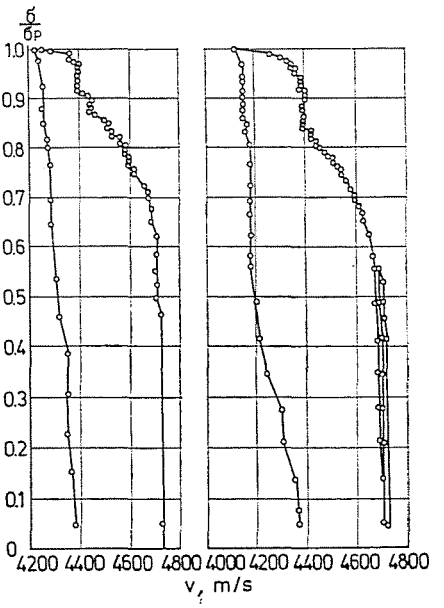

Fig. 5. Virtual ultrasonic deceleration vs. load. Concrete No. 10

Some important results of the tests can be recapitulated as follows:

— The stepped velocity variation diagram permits to conclude that in course of the failure process some energy is concentrated in stress form, to be released abruptly, shock-wise.

— The measurable velocity variation starts much below the ultimate strength, at 50 to 60% as an average.

— In course of unloading, a part of velocity variation vanishes (behaviour similar to elastic deformation — crack closure), the greatest part persists as permanent velocity variation.

— After a load near the ultimate one, not even unloading prevents further velocity variation.

In final account, the presented testing method yields a lot of useful information of processes in the concrete.

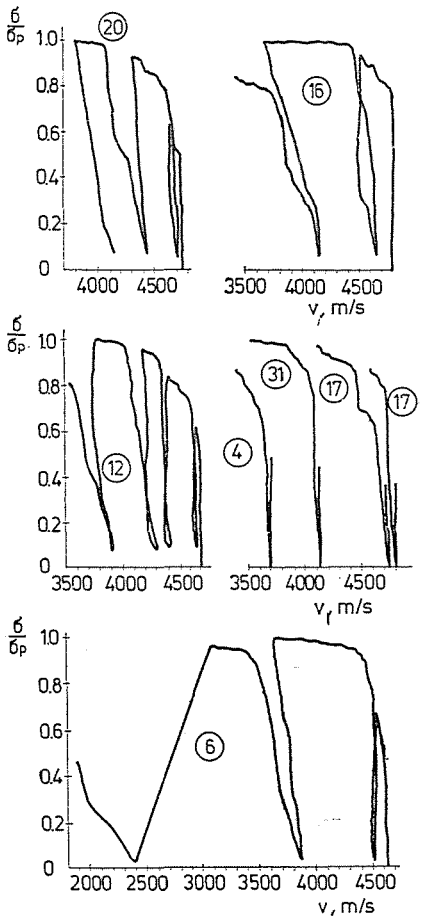

Fig. 6. Typical deceleration diagrams

5. Comparison of results from two methods

Let us point first to the similarity between curves for transversal deformations and for deceleration. Fig. 7 shows deceleration (a) and deformation (b) curves recorded on four differently loaded test specimens as well as those from pickup tests (c). Similarity of curves shows tested phenomena to be identical in both methods. Notice that the ultrasonic measurement is much simpler to apply.

Finally, Fig. 8 is a comparison between results from both methods. Curve in part *a)* is that of average deceleration from all specimens and the deviation from the mean curve (standard deviation). It appears that the variation is sensed by ultrasonic means near 50 to 60% of the ultimate strength. The average volumetric deformation curve in figure *c)* has its maximum about the same stage.

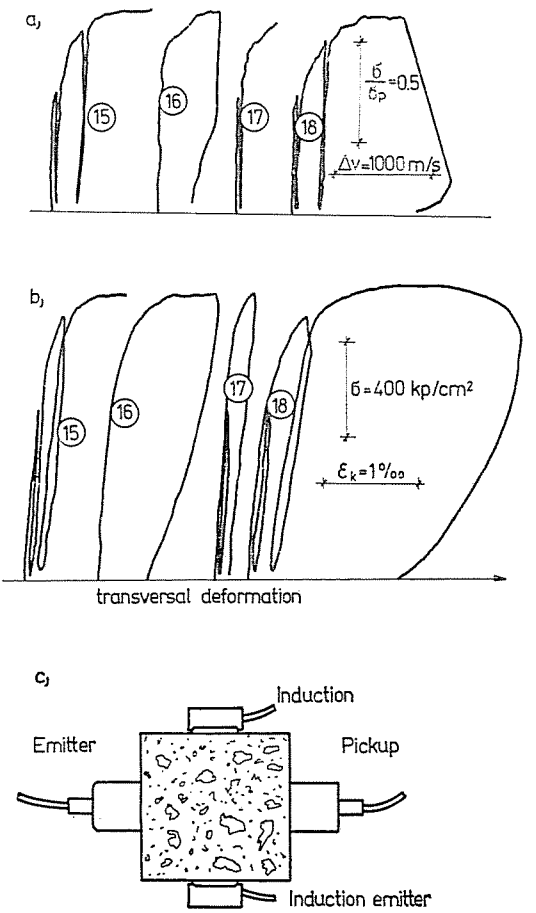

Fig. 7. Comparison between deceleration and deformation curves

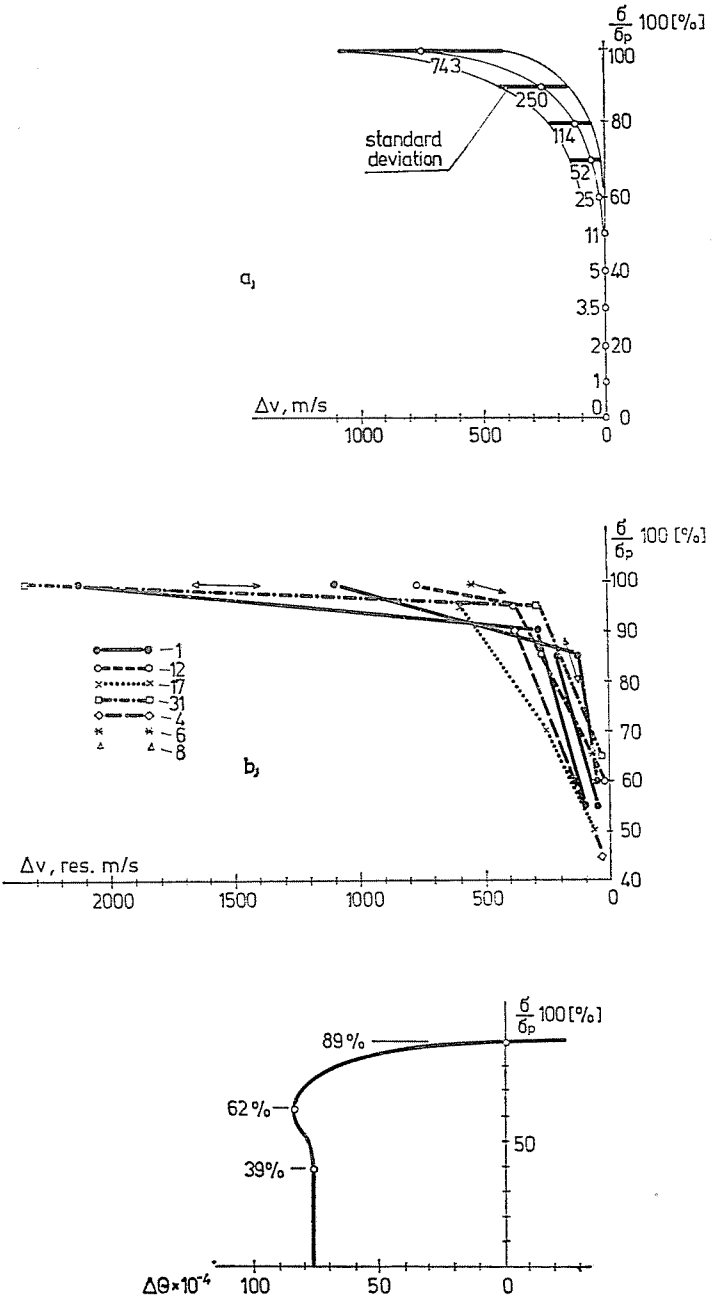

Fig. 8. Comparison between ultrasonic and deformometry results

Permanent velocity variation values of some specimens have been processed in Fig. 8*b*. With increasing load, the permanent deceleration increases, and so does it in unloading after loads amounting to 85 to 95% of the ultimate strength, in agreement with the zero point of the volume increase curve (about 90%).

Thus, both the ultrasonic velocity diagram and the volumetric deformation functions show failure to start at half the ultimate strength to become abrupt at the 0.9th part.

Both methods lend themselves to describe the failure process.

Summary

Concrete prisms have been loaded to or below failure and then unloaded. Simultaneously, longitudinal and transversal deformations have been continuously recorded and plotted as volumetric deformation function of the loaded concrete mass. At the same time variation of the virtual propagation velocity of ultrasonic pulses transversally to the load direction has been determined.

Maxima of volume deformation diagrams of high-strength concretes, hence starting points of deceleration were encountered at about 50 to 60% of ultimate strength, considered as initial observable failure.

Zeros of volume deformation curves are found about where abrupt increase of permanent ultrasonic velocity loss values are noticed, it occurs at about 90% of ultimate strength. This is considered as start of the abrupt advancement of failure. Both methods yield information on the failure of specimens mutually confirming each other.

References

1. Balázs Gy.—Borján J.: High-Strength Gravel Concretes.* Department of Building Materials, Technical University, Budapest, Report No. 14. Közlekedési Dokumentációs Vállalat, Budapest, 1974
2. Béres L.: Methods for Testing Macroscopic Variations of Concrete under Load.* Építés i Kutatás, Fejlesztés. Sept.—Oct. 1968, pp. 6—7
3. Béres L.: Structural Changes in Concrete Due to Loads* FIP, 1968, Oct. pp. 86—90

Dr. György Balázs
József Borján
H-1521 Budapest

* In Hungarian